First principles study of oxygen vacancy migration in tantalum pentoxide

R. Ramprasad
Semiconductor Products Sector, Motorola, Inc., 2100 E. Elliot Road, Tempe, Arizona 85284

(Received 26 August 2003; accepted 5 November 2003)

First principles total energy calculations were performed in order to determine oxygen vacancy migration energies in Ta_2O_5. A simplified version of the crystalline orthorhombic phase of Ta_2O_5 was used in this study. O vacancies in the chosen model of Ta_2O_5 can be broadly classified into 'cap' and 'in-plane' sites based on their location in the lattice. The cap type of vacancies display the largest barriers both for migration to a neighboring cap site or to a neighboring in-plane site, thus behaving as oxygen vacancy 'sinks'. A lowering of the barriers to migration is generally seen when the vacancies are doubly positively charged. All calculations were performed within the local density approximation of density functional theory, and the elastic band method was used in the estimation of migration barriers. © *2004 American Institute of Physics.*
[DOI: 10.1063/1.1637132]

I. INTRODUCTION

Tantalum pentoxide (Ta_2O_5) is one of the high dielectric constant—or 'high-k'—materials that is finding renewed interest primarily due to the ability to deposit it using conventional methods compatible with equipment and processes already available in the semiconductor industry.[1–4] A major concern with most high-k dielectrics, including Ta_2O_5, is their reliability, which is intimately tied to their degradation and breakdown. In fact, there is evidence for an inverse relationship between the dielectric constant and the life time (or 'time to failure') of the dielectrics.[6] One of the factors that could play an important role in the degradation (and to some extent in the leakage behavior) is the electric field assisted migration of defects, particularly oxygen vacancies.

Recently, we reported on a study of oxygen vacancy induced defect states in the band gap of bulk Ta_2O_5.[5] In that study, the atomistic structure of Ta_2O_5 was chosen so that it is computationally tractable, while at the same time representative of deposited films.[7,8] In this chosen model of Ta_2O_5, as in deposited Ta_2O_5 films,[7,8] the basic building blocks were TaO_6 and TaO_7 polyhedra. Based on their location, the O vacancy defects could be broadly classified into two types, each displaying qualitatively different behavior. For instance, the 'in-plane' type of vacancy—shared by 3 polyhedral building blocks—displayed mid gap level occupied states and shallow unoccupied states, while the 'cap' type vacancies—shared by 2 polyhedral building blocks—displayed shallow occupied states. Also, for a wide range of possible values of the electronic chemical potential, 'in-plane' vacancies in the neutral and doubly positive charge states and 'cap' type vacancies in the doubly positive charged state were most stable.

In the present study, the atomistic model of Ta_2O_5 optimized and used in this earlier study is used to determine barriers to O vacancy migration. Several different pathways to migration were explored, and defects in the neutral and doubly positive charge states were considered. We provide details of the calculation methods used in this work in Section II, and the results of the O vacancy migration calculation in Section III.

II. MODEL AND METHOD

An orthorhombic Ta_2O_5 unit cell containing two Ta_2O_5 formula units (4 Ta and 10 O atoms) consisting of two octohedral TaO_6 and two pentagonal bipyramidal TaO_7 polyhedra (Fig. 1) was used in this study.[5] Although this is a simplified version of the actual crystalline phase, the chosen structure shares a number of similarities with the latter as well as with as-deposited Ta_2O_5 films, as demonstrated earlier.[5,7,8] The structure used for the oxygen vacancy calculations was twice the size of the bulk unit cell (containing 8 Ta and 19 O atoms), with the unit cells stacked along the direction perpendicular to the cross section shown on the left of Fig. 1.

All calculations were performed using the local density approximation (LDA) within density functional theory (DFT), as implemented in the Vienna *ab initio* simulation package (VASP),[9] using ultrasoft pseudopotentials. A plane-wave basis set with an energy cutoff of 29 Ry for the wave function and 68 Ry for the electron density was used. The oxygen vacancy calculations were performed with 8 k points in the irreducible wedge of the Brillouin zone. Further doubling the size of the supercell had negligible effects on the vacancy formation energy. All calculations involved relaxation of the atomic positions until the forces on each atom were below 0.04 eV/A.

The migration pathway of the vacancy and the energy barrier to migration were determined by finding the minimum energy path from one lattice site to an adjacent site using a variation of the nudged elastic band (NEB) method[10] as implemented in VASP.[11] First, the two endpoint configurations were determined by separately optimizing the structure with the vacancy at each of the two adjacent sites. A set of intermediate configurations, or 'images', generated by linear interpolation between the two endpoint configurations were then optimized so as to converge to points on the mini-

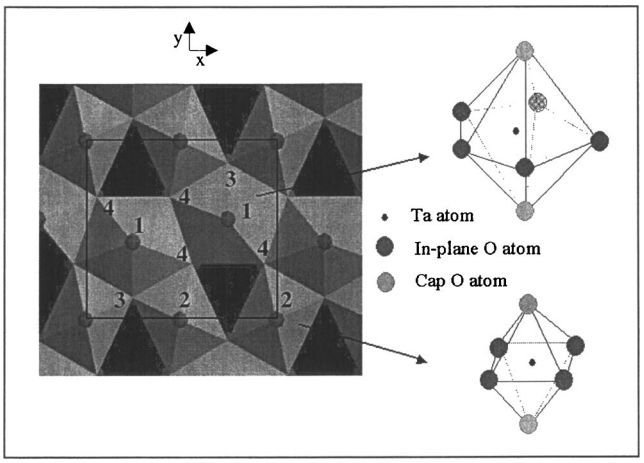

FIG. 1. Schematic of the Ta_2O_5 structure used in the present calculation, with the rectangle highlighting the unit cell. Also shown are perspective views of the TaO_7 (top, right) and TaO_6 (bottom, right) building blocks, with the in-plane and cap site O locations explicitly identified. The 4 symmetry-inequivalent atoms are labeled within the unit cell, with labels 1 and 2 denoting cap sites and labels 3 and 4 denoting in-plane sites. Oxygen vacancy calculations were performed using a structure twice the size of the bulk unit cell, with the two unit cells stacked along the *z*-axis.

mum energy path. Harmonic spring interactions were used to connect the different images of the system along the path, with spring constants chosen to ensure that the distance between the images along the path are maintained constant.[11] A parallel implementation of the VASP code in a Linux cluster was used, with each image assigned to a separate processor. Efficient parallelization was achieved as the total energy calculation of the images along the path are independent of each other. A typical calculation involved eight images along the migration path (excluding the two endpoint configurations). A limited number of calculations were performed using the generalized gradient approximation (GGA); migration energies, being relative energies, followed a trend identical to that of the LDA results, as has been observed earlier both in nudged elastic band calculations of impurity atom migration energies in solids,[12] as well as activation energy calculations in molecular reactions.[13] Owing to this consistency, and the facts that the GGA is not known provide a systematic correction to the LDA migration energy results, that the deficiencies of the LDA are better understood, and that we are primarily interested in general trends in this work, all subsequent calculations were performed using the LDA.

III. RESULTS AND DISCUSSION

Oxygen vacancy sites were classified broadly into two distinct varieties—the 'in-plane' and the 'cap' sites—in our earlier study.[5] The in-plane sites are in the pentagonal or rectangular planes of the TaO_7 and TaO_6 building blocks, respectively, and the cap sites are sites that cap the pentagonal or rectangular planes. Both types of sites are clearly indicated in Fig. 1. Our chosen unit cell consists of two distinct symmetry-inequivalent in-plane (labeled 1 and 2 in Fig. 1) and two distinct cap (labeled 3 and 4) sites. In keeping with our classification of oxygen vacancy sites, we consider three typical oxygen vacancy migration pathways: (i) migration from a cap site to a neighboring cap site, (ii) migration from an in-plane site to a neighboring in-plane site, and (iii) migration from a cap site to a neighboring in-plane site. Also, oxygen vacancies in two different charge states, *viz.*, the neutral and +2 states, were considered. These choices were again motivated by our earlier study,[5] which indicated that the neutral and +2 charge states were the most stable states for a wide range of possible values of the local electrochemical potential. Table I lists the total energies of oxygen vacancy containing supercells with total charges of 0 and +2. All energies for each charge state are relative to the corresponding cap type vacancy containing systems with site label 1.

TABLE I. Total energies of neutral (E^0_{rel}) and +2 charged (E^{+2}_{rel}) oxygen vacancy containing super-cells for various locations of the vacancies; site labels (first column) correspond to labels in Fig. 1, and all energies are relative to the cap type vacancy with site label 1.

Site label	Site type	E^0_{rel} (eV)	E^{+2}_{rel} (eV)
1	cap	0.0	0.0
2	cap	−0.6	0.0
3	in-plane	−0.5	1.2
4	in-plane	−1.2	−0.8

A. Cap site to cap site migration

Figure 2 shows the chosen oxygen vacancy migration path that connects two symmetry-equivalent cap sites with site label 1, and the total energy along this path as calculated using the elastic band method. The circles correspond to actual results of the calculation for each of the minimum energy intermediate configurations or images, and the lines are interpolated. The neutral vacancy clearly displays a large activation barrier (≈5 eV), while the barrier for the +2 charged vacancy is lower by almost an eV. The reason for the barrier lowering is presumably the following: the neutral vacancy has 2 bonding electrons associated with it;[5] removal of these 2 electrons (thereby creating the +2 charged state) results in the surrounding lattice relaxing away from the vacancy. This relaxing makes it easier for the vacancy to migrate, thereby lowering the barrier to migration. Nevertheless, regardless of the charge state, for typical diffusion prefactors of $10^{12}\,\mathrm{sec}^{-1}$,[14] the considered cap site oxygen vacancy migration can be expected to be improbable on the time scale of minutes up to a temperature of about 1500 K. Other cap site migration pathways (site 1 to site 2, or site 2 to site 2) were not considered. The primary reason for this omission is that the total energy differences for systems with an oxygen vacancy at site 1 versus that at site 2 for both charge states is not significant (0.6 eV for the neutral and 0.0 eV for the +2 state, as can be deduced from Table I), and so we expect similar results for these alternative pathways. We wish to mention that the slight asymmetry of the total energy profile about the maximum in Fig. 2 is believed to be a numerical aberration caused by the even number of intermediate configurations or images used along the migration path. Choosing an odd number of images so that one of the images lies close to the transition state, or increasing the number of images will help get rid of the asymmetry.

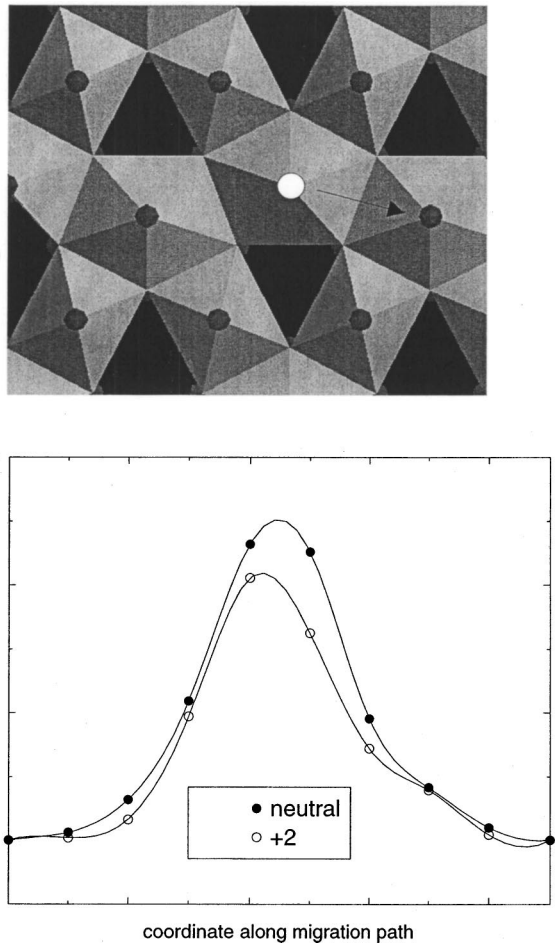

FIG. 2. Above: Migration pathway (indicated by an arrow) connecting two symmetry-equivalent cap sites (site label 1). The white circle represents vacancy location at the starting configuration. Below: Relative total energy along the migration pathway for neutral and +2 charged oxygen vacancies. Symbols represent actual results of the calculation for each of the intermediate configurations or images, and the lines are interpolated. Energies are referenced to the total energy of system at the starting configuration.

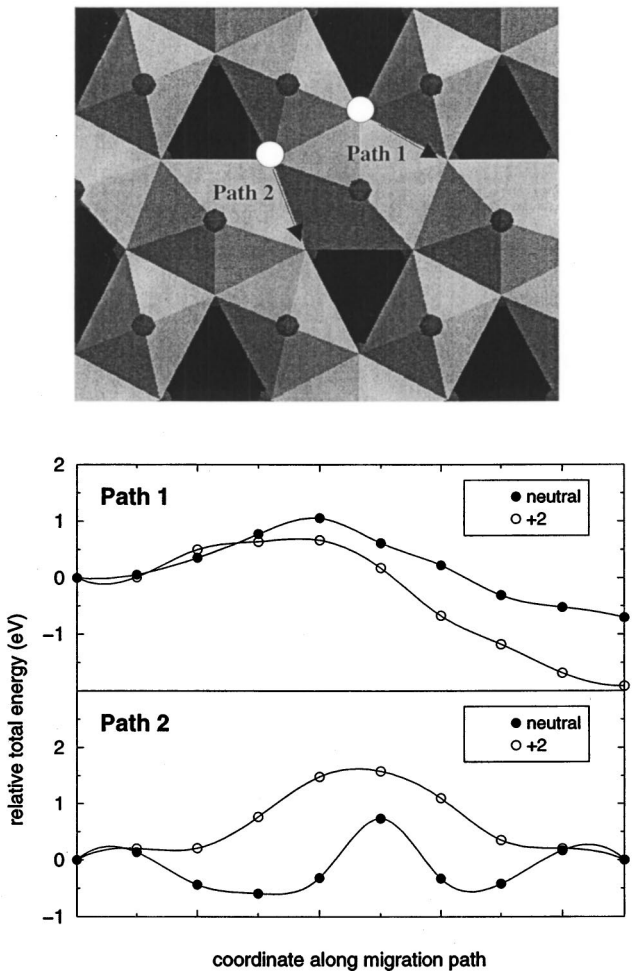

FIG. 3. Above: Migration pathway (indicated by arrows) connecting two symmetry-inequivalent in-plane sites (denoted as path 1 connecting sites 3 and 4), and two symmetry-equivalent in-plane sites (denoted as path 2 connecting two sites with site label 3). The white circles represent vacancy location at the starting configuration for each path. Below: Relative total energy along the migration pathways for neutral and +2 charged oxygen vacancies. Symbols represent actual results of the calculation for each of the intermediate configurations or images, and the lines are interpolated. Energies are referenced to the total energy of system at the starting configuration.

B. In-plane to in-plane site migration

Systems with in-plane vacancies display larger variations in total energy depending on the location of the vacancies. For instance, from Table I, the difference between the total energies of systems with vacancies in sites 3 and 4 is 0.7 eV for the neutral state and 2.0 eV for the +2 state. As a result, we consider two different pathways: a pathway connecting site 3 and site 4 (denoted as path 1 in Fig. 3) and a pathway connecting two adjacent symmetry-equivalent sites with site label 4 (denoted as path 2).

Consider path 1 first. Irrespective of the migration direction, Fig. 3 shows that the activation barrier for the neutral vacancy is ≈1–1.5 eV, much lower than that for cap site to cap site migration in Fig. 2. For the +2 charged vacancy, one of the migration path endpoints is significantly lower in energy than the other, and this manifests as a slight reduction in the activation barrier to migration along the direction from site 3 to site 4. In order to determine if this is an actual barrier lowering, we consider path 2, which connects two equivalent sites. For the case of the neutral vacancy, we see configurations that had previously eluded us that are more stable than the endpoint configurations; these more stable configurations correspond to the minima on either sides of the maximum in the curve for the neutral vacancy in Fig. 3. Such more stable intermediate configurations were not found for the +2 charged vacancy systems, making it hard to compare the activation barriers for the neutral and +2 charged states. Nevertheless, the general conclusion is that the barriers to migration of an oxygen vacancy from an in-plane to in-plane site is much lower than that for cap site to cap site migration.

C. Cap site to in-plane site migration

Finally, we consider oxygen vacancy migration between cap and in-plane sites (Fig. 4). Specifically, we consider the pathway connecting sites 1 and 3. For the neutral case, we see barriers of about 2.5 eV, irrespective of the direction of migration, but for the +2 charged case, there is a large difference in barriers depending on the direction of migration.

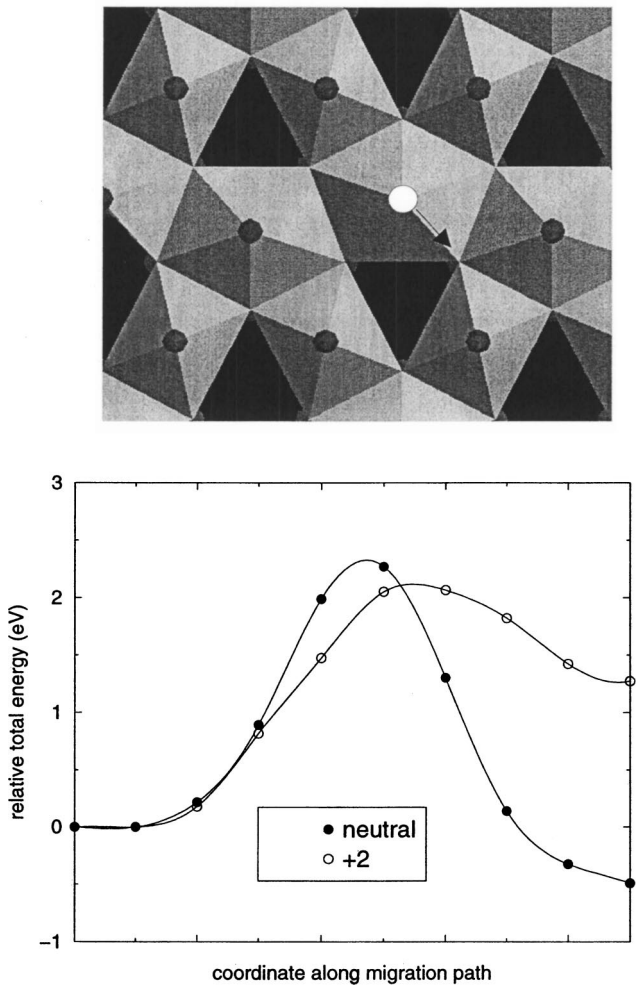

FIG. 4. Above: Migration pathway (indicated by an arrow) connecting a cap site (site label 1) and an in-plane site (site label 3). The white circle represents vacancy location at the starting configuration. Below: Relative total energy along the migration pathway for neutral and +2 charged oxygen vacancies. Symbols represent actual results of the calculation for each of the intermediate configurations or images, and the lines are interpolated. Energies are referenced to the total energy of system at the starting configuration.

For instance, an approximately 2 eV barrier is seen for the cap to in-plane site, whereas an approximately 0.7 eV barrier is seen for the opposite direction. Also, as in the cap site to cap site migration case, a clear barrier lowering is seen for +2 charged vacancy migration irrespective of migration direction.

Thus, while a rich variety of stable oxygen vacancy configurations and migration energies are displayed in Ta_2O_5, the general conclusion we arrive at is that cap sites serve as oxygen vacancy 'sinks', in the sense that vacancies arriving at these type of sites can be expected to be subsequently immobile.

IV. SUMMARY

Density functional total energy calculations combined with the elastic band method were used to determine oxygen vacancy migration energies in Ta_2O_5. A previously optimized model of crystalline orthorhombic Ta_2O_5 was used in this study. Oxygen vacancies in the chosen model of Ta_2O_5 can be broadly classified based on their coordination environment into cap and in-plane sites. The cap site vacancies display the largest barriers both for migration to a neighboring cap site or to a neighboring in-plane site. The cap type vacancies thus behave as oxygen vacancy 'sinks', as vacancies arriving at these sites can be expected to be subsequently immobile under typical experimental conditions. Vacancies in two charged states (neutral and +2) were considered in this study. A lowering of the barriers to migration is seen in many cases when the vacancies are doubly positively charged.

ACKNOWLEDGMENTS

The author would like to acknowledge helpful discussions with Tom Remmel and Mike Petras. Mike Petras and Mel Miller are also acknowledged for critically reading the manuscript.

[1] C. Chaneliere, J. L. Autran, R. A. B. Devine, and B. Balland, Mater. Sci. Eng. R **22**, 269 (1998).
[2] C. C. Barron, T. P. Remmel, D. R. Roberts, M. V. Raymond, E. D. Luckowski, S. Kalpat, M. Sadd, P. Zurcher, R. Ramprasad, and M. Miller, Proceedings of the 202nd Electrochemical Society (October, 2002).
[3] D. R. Roberts, S. Kalpat, T. P. Remmel, M. A. Sadd, M. V. Raymond, R. Ramprasad, E. D. Luckowski, and M. Miller, Proceedings of the 202nd Electrochemical Society (October, 2002).
[4] R. M. Fleming *et al.*, J. Appl. Phys. **88**, 850 (2000).
[5] R. Ramprasad, J. Appl. Phys. **94**, 5609 (2003).
[6] J. McPherson, J. Kim, A. Shanware, H. Mogul, and J. Rodriguez, Proceedings of the International Electron Devices Meeting (November, 2002).
[7] N. C. Stephenson and R. S. Roth, Acta. Cryst. B **27**, 1037 (1971).
[8] Hidekazu Kimura, Junichiro Mizuki, Satoshi Kamiyama, and Hiroshi Suzuki, Appl. Phys. Lett. **66**, 2209 (1995).
[9] G. Kresse and J. Hafner, Phys. Rev. B **47**, 558 (1993); G. Kresse and J. Furthmuller, Phys. Rev. B **54**, 11169 (1996).
[10] G. Mills, H. Jonsson, and G. K. Schenter, Surf. Sci. **324**, 305 (1995); G. Henkelman and H. Jonsson, J. Chem. Phys. **113**, 9978 (2000).
[11] See the VASP manual at http://cms.mpi.univie.ac.at/vasp/vasp/vasp.html
[12] W. Windl, M. M. Bunea, R. Stumpf, S. T. Dunham, and M. P. Masquelier, Phys. Rev. Lett. **83**, 4345 (1999).
[13] R. Ramprasad, Ph.D. Dissertation, *Density Functional Study of Automotive Catalysis* (University of Illinois, Urbana-Champaign).
[14] G. L. Kellog, Surf. Sci. Rep. **21**, 1 (1994).